A SOSEKI-based coordinate system interprets global polarity cues in *Arabidopsis*

Saiko Yoshida [1,2,4]*, Alja van der Schuren [1,5,8], Maritza van Dop[1,8], Luc van Galen[1], Shunsuke Saiga[1,6], Milad Adibi[3], Barbara Möller[1,7], Colette A. ten Hove[1], Peter Marhavy[2,5], Richard Smith[3], Jiri Friml [2] and Dolf Weijers [1]*

Multicellular development requires coordinated cell polarization relative to body axes, and translation to oriented cell division[1–3]. In plants, it is unknown how cell polarities are connected to organismal axes and translated to division. Here, we identify *Arabidopsis* SOSEKI proteins that integrate apical–basal and radial organismal axes to localize to polar cell edges. Localization does not depend on tissue context, requires cell wall integrity and is defined by a transferrable, protein-specific motif. A Domain of Unknown Function in SOSEKI proteins resembles the DIX oligomerization domain in the animal Dishevelled polarity regulator. The DIX-like domain self-interacts and is required for edge localization and for influencing division orientation, together with a second domain that defines the polar membrane domain. Our work shows that SOSEKI proteins locally interpret global polarity cues and can influence cell division orientation. Furthermore, this work reveals that, despite fundamental differences, cell polarity mechanisms in plants and animals converge on a similar protein domain.

Development of multicellular organisms relies on the ability to organize cell differentiation and division relative to body axes and to other cells in the same tissue. Individual cells are polarized, and polarity information is relayed to trigger local outgrowth[1,2] or steer division orientation[1,3]. Mechanisms underlying polarization and division orientation are relatively well-understood in yeast and animals[4,5]. In plants, oriented division is critical for normal development[6,7], and several polarly localized proteins have been identified[8–15]. However, yeast and animal polarity regulators seem to be missing from plant genomes, and it is thought that polarity components and mechanisms are distinct in plant and animal kingdoms[16]. Components of such mechanisms are elusive. The plant signalling molecule auxin regulates pattern formation, and defects in auxin response often manifest as changes in growth direction or cell division plane[6,17]. Mutations in the *Arabidopsis* MONOPTEROS/ AUXIN RESPONSE FACTOR5 transcription factor[18] cause alterations in division planes in the early embryo[19]. We argued that mediators of MONOPTEROS function in controlling cell division orientation should be among its transcriptional targets. Starting from a set of MONOPTEROS-dependent genes[20], we here identify a family of unique, polarly localized proteins that link organismal axes to cell polarity and division orientation.

We previously performed transcriptome analysis on globular-stage embryos in which MONOPTEROS activity was locally inhibited[20], and identified *TMO7*[21] as the most strongly down-regulated gene[20]. The second most strongly down-regulated gene (7.5-fold) is a gene of unknown function, containing a Domain of Unknown Function 966 (DUF966) and named *SOSEKI1* (explained below; *SOK1*; At1g05577). *SOK1* has four paralogues in the *Arabidopsis* genome: *SOSEKI2* (*SOK2*; At5g10150), *SOSEKI3* (*SOK3*; At2g28150), *SOSEKI4* (*SOK4*; At3g46110) and *SOSEKI5* (*SOK5*; At5g59790) (Fig. 1a and Supplementary Fig. 1) of which *SOK5* was also 2.4-fold down-regulated in embryos with reduced MONOPTEROS function.

To determine gene expression domains, nuclear-localized triple green fluorescent protein (GFP) (n3GFP) was driven by each *SOK* promoter, and this revealed that all *SOK* genes are expressed during embryogenesis and in primary/lateral roots (Supplementary Fig. 2). To observe protein localization, C-terminal YFP translational fusions were generated. All SOK-YFP patterns mirror pSOK-n3GFP patterns (Figs. 1 and 2 and Supplementary Fig. 2). Each SOK protein marked novel cellular domains. SOK1-YFP marks the outer/apical edge of young vascular cells, including the pericycle, and the columella root cap in the primary root (Fig. 1b,c,h). During embryogenesis, SOK1-YFP is first detected in the apical side of lower tier inner cells at the early globular stage (Fig. 2a). Subsequently, SOK1 localizes to the outer apical corner or outer lateral side of vascular cells and outer corners of the hypophysis at transition to heart stage (Fig. 2f, Supplementary Video 1 and Supplementary Fig. 3). This pattern is maintained in the post-embryonic root (Fig. 1) and the lateral root (Fig. 2k and Supplementary Fig. 4). The same localization pattern was observed for SOK1-tdTomato (Supplementary Fig. 2), and is hence independent of the protein tag. The protein was named SOSEKI1 (Japanese for 'cornerstone') for this unique corner localization pattern. The SOK1 protein is highly unstable: SOK1-YFP signal disappears during cell division but is afterwards quickly re-established in lateral root primordia (Fig. 2p and Supplementary Video 2) and primary root (Fig. 2q and Supplementary Video 3). Treatment of SOK1-YFP roots with the translation inhibitor Cycloheximide (CHX) confirmed protein instability (Supplementary Fig. 6).

All other SOK proteins were localized to different subcellular edges. SOK2-YFP localized to the inner basal edge of endodermal cells in the primary (Fig. 1d,i) and lateral root (Fig. 2l and
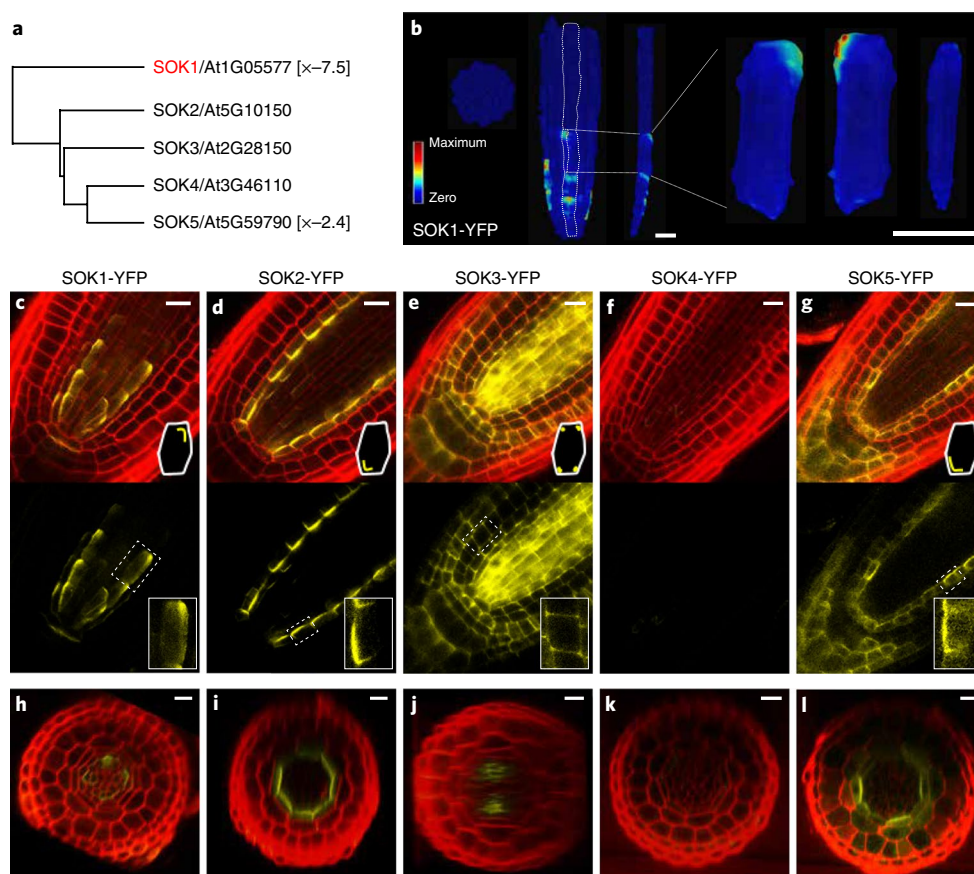
Fig. 1 | The SOSEKI family of polarly localized proteins. a, Phylogenetic tree of the *Arabidopsis* DUF966/SOSEKI protein family. Values in brackets indicate fold-change (down-regulation) in Q0990»bdl embryos[20]. **b**, SOK1-YFP protein localization in a root tip. Fluorescence values are shown in false colour (red = maximum; blue = zero) on segmented cell surfaces. From left to right: cross-section of vascular cylinder, surface view of vascular cylinder, single cell file and three different views of a single segmented cell. **c–l**, Localization of SOK1-YFP (**c,h**), SOK2-YFP (**d,i**), SOK3-YFP (**e,j**), SOK4-YFP (**f,k**) and SOK5-YFP (**g,l**) in longitudinal cross-sections (**c–g**) and transverse cross-sections (**h-l**) of primary root meristems counterstained with propidium iodide (red). Insets in **c,d,e,g** schematically show subcellular SOK protein localization (top), and magnification of localisation in a single cell (bottom). Scale bars, 10 μm. All sample and observation numbers are listed in Supplementary Table 3.

Supplementary Fig. 4), starting in the globular embryo (Fig. 2b and Supplementary Fig. 3). SOK3-YFP accumulated at the basal side and all corners of most cells in the primary root (Fig. 1e,j), lateral roots (Fig. 2m and Supplementary Fig. 4) and embryos (Supplementary Fig. 3). Only faint SOK4-YFP accumulation was observed few vascular cells in the primary root (Fig. 1f,k), while it was expressed in lateral root (Fig. 2n and Supplementary Fig. 4) and embryo (Fig. 2d,i and Supplementary Fig. 3). SOK5-YFP resembles SOK2 localization in endodermis, QC and lateral root cap in primary root (Fig. 1g,l), yet SOK2 and SOK5 patterns differ during embryogenesis (Fig. 2e,j and Supplementary Fig. 3). Thus, all SOK proteins are expressed in specific tissues during root initiation, growth and branching, and mark unique polar subcellular domains.

To test whether differences in polar localization among SOK proteins are caused by cell types or protein determinants, we mis-expressed SOK1-YFP or SOK2-YFP from the *RPS5A* promoter that drives broad expression in meristems[22]. Apical SOK1 polarity was found in all cell types, but mis-expressed SOK1 localizes to inner rather than outer edges in cortex and epidermis (Fig. 3a–c). Ectopic SOK2-YFP localizes to inner basal edges of all cells (Fig. 3e). Thus apical/basal polarity is maintained in mis-expression lines and appears intrinsic to SOK1 and SOK2 proteins. In these lines, polar localization was found across the embryonic shoot/root axis (Fig. 3d,f), suggesting the existence of a common polarity reference in the entire body. During lateral root initiation, however, localization

followed the new organ axis (Fig. 2k,l and Supplementary Fig. 4), suggesting that the SOK-based coordinate system is autonomous to lateral organs. In contrast to apical/basal polarity, inner/outer polarity of SOK1 depended on position relative to the endodermis (Fig. 3a); SOK1 always localized pointing towards the endodermis. Localization in the *shortroot* (*shr*) and *scarecrow* (*scr*) mutants with impaired endodermal identity[23,24] caused loss of edge localization and led to apical accumulation in the mutant cell file (Fig. 3k,l). This suggests that edge localization integrates genetically separable apical–basal and outer–inner axes. The cortex–endodermis junction serves as a potent cue for SOK1 localization, which is confirmed by ground tissue-specific expression of SOK1-YFP using the N9135 GAL4 driver line[25]. In the shared initial for cortex/endodermis, SOK1-YFP is apical, while the protein localized at both opposing edges toward the junction after the periclinal division separating separates endodermis and cortex (Fig. 3m,n). These observations revealed that plant cells and tissues possess a universal coordinate system with an internal reference that is read and integrated by SOK proteins. While other proteins, such as BOR1 can use this internal reference system[26,27], it is unclear if other proteins can likewise integrate axes.

Polar localization of plant proteins generally depends on dynamic processes such as membrane trafficking, cytoskeletal dynamics or protein degradation[8–10,12,14]. In stark contrast, none of 20 tested hormone or drugs affecting these processes, or changes in light, temperature or gravity angle affected the edge localization of
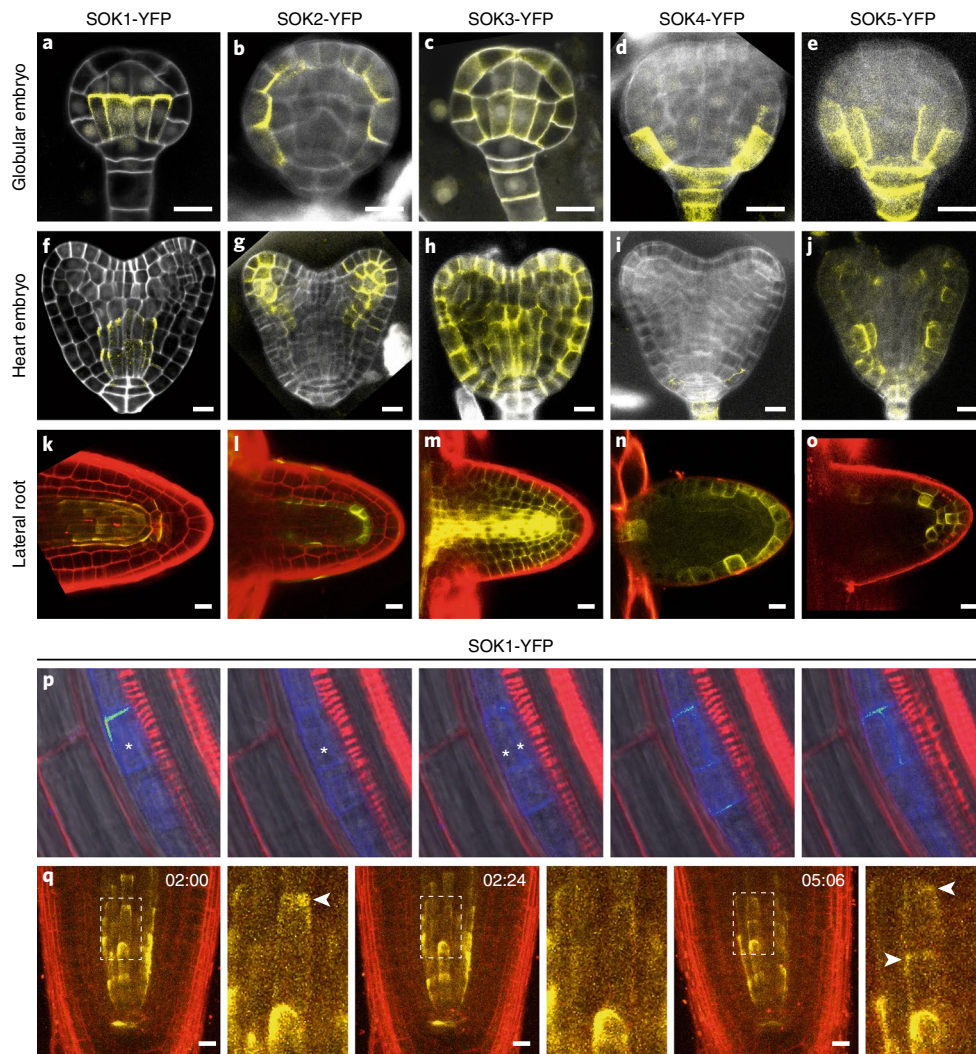
Fig. 2 | Diverse polar patterns of SOSEKI proteins. a–o, Localization of SOK1-YFP (**a,f,k**), SOK2-YFP (**b,g,l**), SOK3-YFP (**c,h,m**), SOK4-YFP (**d,i,n**) and SOK5-YFP (**e,j,o**) in globular-stage embryos (**a–e**), heart-stage embryos (**f–j**) and emerged lateral root primordia (**k–o**). **p,q,** Stills of a time-lapse imaging series of SOK1-YFP fluorescence in an initiating lateral root (**p**) and in the primary root tip (**q**). In **p**, the left panel corresponds to the start of the observation, and subsequent images were taken 1, 2, 3 and 4 hours later. Dividing cell lineages are marked with asterisks. In **q**, time (in hours) from the start of the experiment is given in each panel. In **q**, a dividing cell is magnified from the region indicated by a dashed box, and SOK1-YFP signal is indicated by arrowheads. Embryos in **a–j** are counterstained with Renaissance RS2200 (white), and roots (**k–q**) with propidium iodide (red). Scale bars, 10 μm. All sample and observation numbers are listed in Supplementary Table 3.

SOK1, SOK2 or SOK3 (Supplementary Fig. 6 and Supplementary Table 1). This suggests that polar localization follows a pathway that is different from well-known polar proteins such as PINs, BOR1, NIP5 and PEN3[8–10,12,14]. We next tested whether the cell wall or mechanical properties influence SOK localization and found that a brief (<20 min) treatment with cell wall-degrading enzymes or high osmotic mannitol solution led to internalization and mis-localization of SOK proteins (Fig. 3o–q and Supplementary Fig. 5). This indicates that cell-wall integrity is critical for edge localization and membrane association of SOK proteins.

SOK1-YFP mis-expression induced frequent alterations in cell division orientation; in embryos, such divisions were found in all cell types (Fig. 3i,j and Supplementary Fig. 7), while in roots, defects were strongest in the cortex and epidermis (Fig. 3a,g,h). While root cells normally divide anticlinal to the growth axis (Fig. 3g), mis-expression lines showed either oblique or periclinal divisions generating additional cell layers (Fig. 3h). The same defect was induced by mis-expressing non-tagged SOK1, and was accompanied by slightly inhibited root growth (Supplementary Fig. 7). We used

this activity in redirecting cell division planes to determine protein determinants and properties required for activity. SOK proteins do not have a signal peptide or predicted transmembrane helices (Supplementary Fig. 1) and are probably peripherally membrane-associated. To target SOK1 uniformly to the plasma membrane, we fused an N-terminal Myristoylation (Myr) motif[28] to SOK1-YFP. Both polarity and activity (as judged by oblique cell divisions) were strongly diminished in Myr-SOK1-YFP roots (Fig. 3r). In contrast, when the same Myr motif was fused to the C-terminus of SOK1-YFP as a negative control, neither polarity nor activity was affected (Fig. 3s). Thus, insertion in the plasma membrane prevents polar localization, which is in turn required for SOK1 function.

To locate polarity determinants, we generated a series of N- or C-terminal deletions (Fig. 4a–e and Supplementary Fig. 8) and mis-expressed each as a YFP fusion. Deletions ΔA, ΔB, ΔC and ΔD caused SOK1 to be localized in the cytosol. ΔE localized to the apical edge and induced oblique divisions (Fig. 4c), suggesting that the fragment contained in the ΔD-ΔE segment is sufficient for polar localization and for altering division orientation. Deletions ΔF, ΔG, ΔH
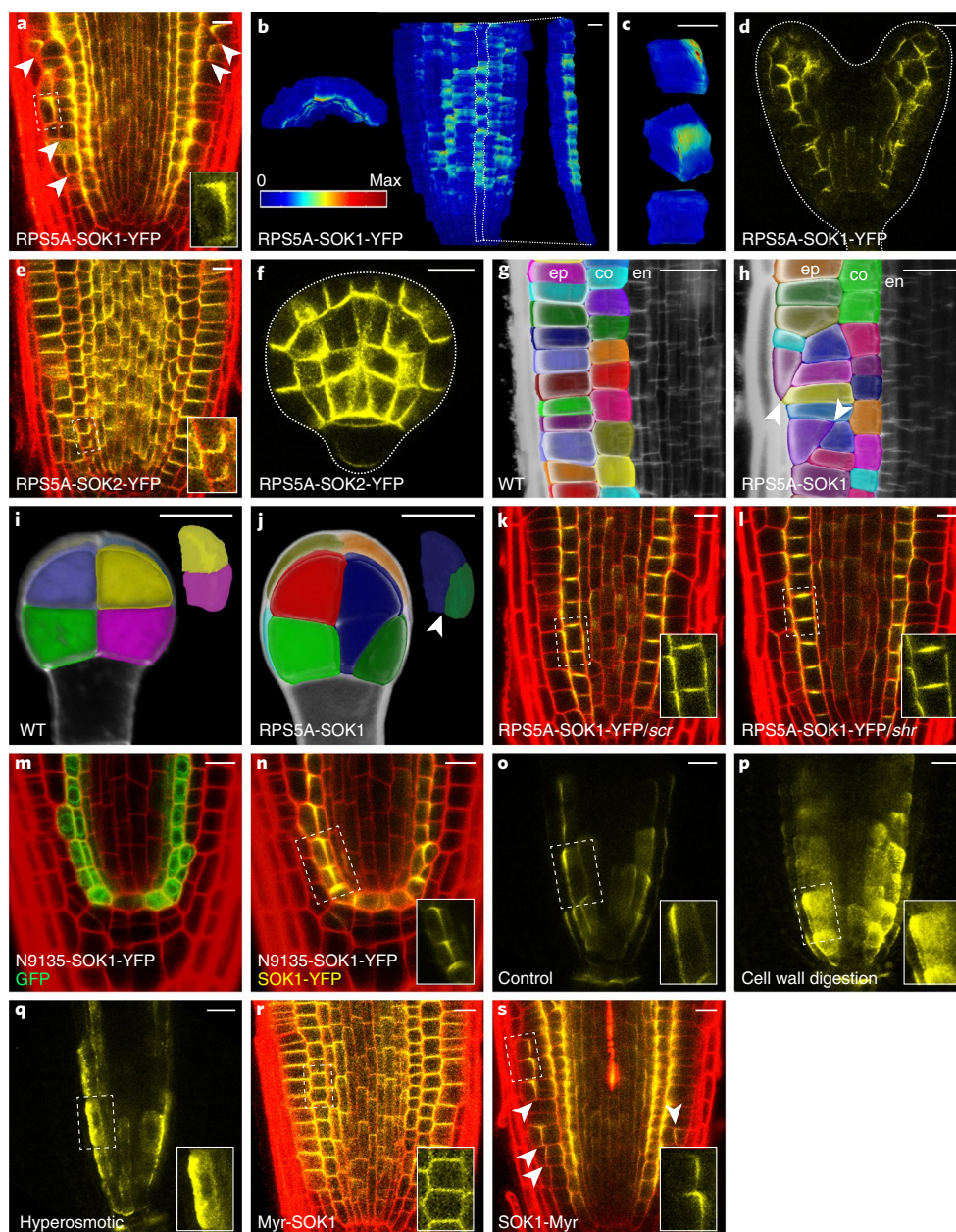
Fig. 3 | Regulation of SOSEKI localization. a, Localization of SOK1-YFP in RPS5A-SOK1-YFP root tip. Arrowheads indicate examples of oblique cell divisions. **b,c,** SOK1-YFP protein localization in a RPS5A-SOK1-YFP root tip (**b**) and three-dimensional (3D) localization of SOK1-YFP on segmented epidermal cells (**c**). Fluorescence values are shown in false colour (red = maximum; blue = zero) on segmented cell surfaces. **d,** SOK1-YFP localization in RPS5A-SOK1-YFP heart stage embryo. **e,f,** Localization of SOK2-YFP in RPS5A-SOK2-YFP root tip (**e**) and globular-stage embryo (**f**). **g–j,** Segmented cell volumes in wild-type (**g,i**) and RPS5A-SOK1 (**h,j**) root meristem (cells located between 70–160 μm away from the quiescent centre were observed in **g,h** and eight-cell embryo in **i,j**. ep, epidermis; co, cortex; en, endodermis. **k,l,** Localization of *RPS5A*-driven SOK1-YFP in *scr* ((**k**) and *shr* (**l**) root tips. **m,n,** GAL4-driven GFP expression (**m**) and GAL4-driven SOK1-YFP accumulation (**n**) in root tip of N9135»SOK1-YFP. **o–q,** Localization of SOK1-YFP in control-treated root tip (**o**) and in root tips treated with cell wall-digesting enzymes for 3 min (**p**) or with 0.4 M mannitol for 1.5 h (**q**). **r,** Myr-SOK1-YFP localization in RPS5A- Myr-SOK1-YFP root tip. **s,** SOK1-Myr-YFP localization in RPS5A-SOK1-Myr-YFP root tip. Arrowheads indicate oblique cell divisions. Walls in **a,e,g–n,r,s** are counterstained with propidium iodide (red in **a,e,k–n,r,s**; gray in **g,h**). Insets in **a,e,k,l,n–s** show SOK protein localization in single cells corresponding to the area in dashed box. Scale bars, 10 μm. All sample and observation numbers are listed in Supplementary Table 3.

and ΔI are broadly localized to plasma membrane, suggesting that the N-terminus is not required for localized membrane association per se, but rather for focusing to the edge. Deletions ΔJ, ΔK and ΔL were all localized to the cytosol, suggesting that the ΔD-ΔE segment can only direct edge localization if the N-terminus is present. Thus, SOK1 carries two function domains: one for membrane association (middle), and another (N-terminal) for focused polar localization. Both are required for activity in changing division orientation.

To test whether different SOK proteins use similar domains for localization, we replaced successive 50–70 amino acids of the basally localized SOK2-YFP by the corresponding region of SOK1 (Named S2S1A-F; Fig. 4f–j and Supplementary Fig. 8). While most chimaeras localized to the basal edge (Fig. 4g,j and Supplementary Fig. 8), S2S1D shifted to the apical edge (Fig. 4h and Supplementary Fig. 8), similar to SOK1-YFP. The S1S2E showed a mixture of SOK1 and SOK2 localization, at the inner lateral membrane (Fig. 4i and
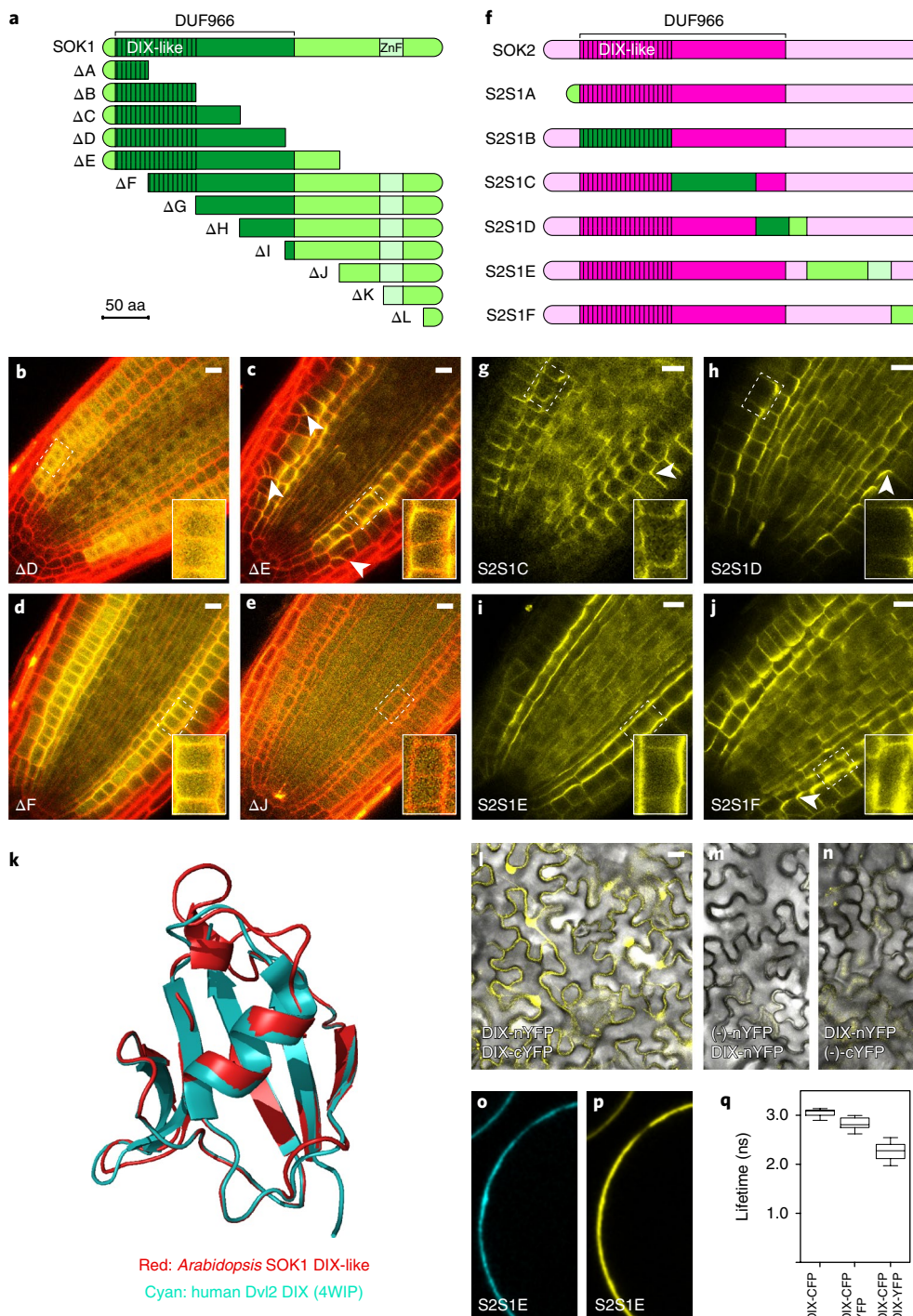
Fig. 4 | Protein determinants for SOK localization and activity. a, Schematic of SOK1 protein domains (ZnF, Zn-finger), and outline of domain deletion constructs expressed as YFP-fusions driven from the *RPS5A* promoter. **b–e**, Representative examples of SOK1-YFP domain deletion accumulation in root tips. Arrowheads in **c** indicate examples of oblique divisions. **f**, Outline of SOK2-SOK1 domain swaps, expressed as YFP-fusions driven from the *RPS5A* promoter. **g–j**, Representative examples of SOK1-SOK2-YFP domain swap accumulation in root tips. Arrowheads in **g** and **j** mark basal localization, arrowhead in **h** marks apical localization. **k**, Structural alignment of the DIX domain in human DVL2 (PDB: 4WIP; blue) and the homology model of the SOK1 DIX-like domain (red). **l**, Bimolecular fluorescence complementation in *Nicotiana benthamiana* epidermis of the SOK1 DIX-like domain in homo-dimeric conformation, using C-terminal YFP fragments. **m,n**, Bimolecular fluorescence complementation (BiFC) control experiments with the DIX-like domain fused only to the N-terminal (**m**) or C-terminal (**n**) YFP half. **o,p**, Fluorescence of co-expressed SOK1 DIX-like domain as CFP (**o**) and YFP (**p**) fusion in protoplast. **q**, Quantification of CFP fluorescence lifetime (in picoseconds, ps) in SOK1-DIX-CFP/YFP pair, and the two individual fusions in protoplasts. Boxplots represent values between upper and lower quartile, with median value shown and error bars representing standard deviation. Walls in **b–e** are counterstained with propidium iodide (red). Scale bars, 10 μm. Insets in **b–e,g–j** show SOK protein localization in single cells corresponding to the area in dashed box. All sample and observation numbers are listed in Supplementary Table 3.

Supplementary Fig. 8). Thus, polar localization can be transferred between SOK1 and SOK2 using a discrete domain that overlaps with the ΔD–ΔE 'polarity domain' defined by deletions. SOK1 mis-expression induces oblique divisions (Fig. 3a), while SOK2 mis-expression does not (Fig. 3e). Even when relocated to the SOK1 polarity domain, SOK2 can not alter division orientation (Fig. 4h). Thus, SOK proteins differ from one another not only in their polar localizations, but also in their ability to modify cell division orientation. We finally confirmed that the same domain conferred polarity changes in swaps between SOK1 and SOK5 (Supplementary Fig. 9). This identifies a minimal domain for polar targeting of multiple SOK members. This minimal polarity domain acts in conjunction with the conserved N-terminal domain to direct focused, polar membrane localization to specific cell edges.

SOK proteins are plant-specific, and the function of DUF966 domain is unknown. We used structural homology modelling to identify potential homologues and found that, despite very low sequence conservation, a part of the DUF966 domain resembles the DIX (Disheveled/Axin) domain (Fig. 4k) that is found in a number of animal proteins[29,30]. The DIX domain mediates head-to-tail oligomerization[31] and is required for clustering of the polarity regulator Disheveled in *Drosophila*[30,31]. Strikingly, the DIX domain is found only in a small number of metazoan proteins, each of which is involved in Wnt signalling and/or planar cell polarity[29,30], which suggests a convergence of polarity mechanisms across kingdoms. We tested the ability of the DIX-like domain in SOK1 to self-associate. Indeed, bimolecular fluorescence complementation in tobacco leaves (Fig. 4l–n) and a Förster resonance energy transfer (FRET) assay in *Arabidopsis* protoplasts (Fig. 4o–q) showed that the predicted DIX domain homodimerizes. The DIX-like domain corresponds to the N-terminal region that is required for edge localization and biological activity (Fig. 4a,d and Supplementary Fig. 1). Thus, the animal cell polarity protein Disheveled and SOSEKI1 may use a homologous protein domain for their asymmetric localization and polarity-related function.

Our study identified a novel plant-specific family of polar, edge-localized proteins. Localization to previously unidentified polar domains is important for the activity of SOK1 in influencing the cell division axis. Whether SOK1 and other family members mediate this function during normal development, and what cellular mechanism underlies such activity is yet to be determined, in part through analysing loss-of-function mutants. Single mutants in individual *SOK* genes did not so far reveal phenotypes (not shown), but redundancy is probable. Thus, current efforts are aimed at generating complete knockout of all family members. Nevertheless, our analysis of SOK localization identified a universal coordinate system in plants that extends well beyond the global polarity field in the leaf[32] and encompasses the entire body axis. SOK proteins that can locally interpret and integrate the global coordinates. Consistent with being the output of a coordinate system, SOK localization is robust, yet seems to rely on cell wall integrity and/or mechanical properties. Further exploration of the mechanisms of SOK localization and function may help revealing the fundamental principles of cell and organismal polarity in plants. This may herald surprising analogies to animal polarity mechanisms, given the adoption of a homologous protein domain in polar proteins across kingdoms.

Methods

Plant material. *Arabidopsis* ecotype Columbia-0 was used in all experiments except when noted otherwise. The N9135-GAL4 enhancer trap line[25] was generated by Jim Haseloff (University of Cambridge) and obtained through the *Arabidopsis* Biological Resource Centre (ABRC). *shr*-2 and *scr*-4 mutants were previously described[33,34].

All seeds were sterilized, sown on Murashige and Skoog medium with 1% sucrose and 0.8% Daishin agar (Duchefa) and vernalized for one day. Plants were grown on soil at 22 °C under the long-day condition.

Molecular cloning. All cloning was performed using previously described ligation-independent cloning methods and vectors[35]. For promoter-GFP lines, 1.2–5 kilobase (kb) fragments upstream of the ATG of *SOK* genes were amplified and introduced into upstream of SV40-n3eGFP in pPLV04. For C-terminal translational fusion lines, genomic fragments, including 1.2–5 kb upstream of *SOK* genes, were introduced into pPLV16 (sYPF2) or pPLV22 (tdTomato). For mis-expression lines, *SOK* complimentary DNAs were amplified, fused with sYFP2 and introduced into pPLV28 downstream of the *RPS5A* promoter. For gene swap experiments, cDNA fragments of *SOK1*, *SOK2*, *SOK5* and YFP were amplified, fused by overlap extension PCR and introduced downstream of the *RPS5A* promoter in pPLV28. For deletion experiments, cDNA fragments from SOK1-YFP were amplified and introduced downstream of the *RPS5A* promoter in pPLV28. For myristoylated SOK1 constructs, sequences for myristoylation (GGCFSKK)[28] was added to either the C- or N-terminus of SOK1 cDNA sequences, and introduced downstream of the *RPS5A* promoter in pPLV28. The *UAS*::SOK1-YFP construct was generated by amplifying SOK1-YFP from the pRPS5A::SOK1-YFP plasmid and introducing it downstream of the GAL4-dependent *UAS* promoter[36] in pPLV32. The construct was transformed directly into the N9135 enhancer trap line[25]. For BiFC, the DIX cDNA sequence was amplified from the pRPS5A::SOK1-YFP plasmid and cloned into a modified pGreenII vector containing p35S::LIC-n/cYFP. Fluorescence lifetime imaging (FLIM) vectors were generated by cloning the DIX cDNA into pMON 35S::LIC-sYFP or pMON 35S::LIC-sCFP3a.

All constructs were sequenced, and transformed into wild-type Columbia or N9135 GAL4 by floral dip using Agrobacterium strain GV3101(pSoup). All primers used for cloning are listed in the Supplementary Table 2.

Microscopic analysis. Roots were stained by propidium iodide (Sigma-Aldrich) at final concentration of 10 µg ml^{-1}. Embryos were fixed and stained by 2.2% Renaissance RS2200 (Renaissance Chemicals) in PBS buffer at pH 6.9 containing 4% paraformaldehyde, 5% glycerol, 4.2% dimethyl sulfoxide (DMSO) or stained by propidium iodide after fixation as previously described[6,37].

Confocal imaging was performed with Zeiss LSM700/800 (observation of lateral root) or Leica SP5/II (observation of primary root and embryo) as previously described[37]. Live imaging was performed with LSM700 as described before[38,39]. For the 3D imaging of pSOK1-SOK1-YFP and pSOK1-GFP root, Zeiss LSM780 with two-photon laser (960–990 nm) and 500–550 nm/575–610 nm band-pass filter were used. Analysis of confocal images (3D reconstruction, 3D segmentation) was performed by MorphoGraphX[40].

Chemical treatments. All chemicals used to treat SOK-YFP roots are shown in Supplementary Table 1. Concentration for each chemical was obtained from literature. Seedlings were placed on Murashige and Skoog plates containing each chemicals for the durations mentioned in the text and were subsequently imaged by confocal microscopy. As controls for the chemical treatments, the same percentage of DMSO or ethanol used for each chemical treatment were used and no effect was observed. For most of the chemical treatments, final concentrations of DMSO were <0.5% (v/v) and ethanol were <0.1% (v/v).

Plasmolysis was performed either on Murashige and Skoog medium with mannitol (Sigma, M9546) at final concentration 0.4 M or by dipping roots in 0.4 M mannitol solution in milliQ water, and stained by FM4-64 at least for 2 min. For cell wall digestion, either 1% Cellulose R10 (Yakult Honsha) and/or 0.2% Macerozyme (Duchefa) were used. Cellulose and/or Macerozyme was dissolved in a solution containing 0.4 M mannitol, 10 mM CaCl2, 20 mM KCl and 20 mM MES (pH 5.7).

BiFC and FRET-FLIM. BiFC was performed as follows: *Agrobacterium* containing BiFC plasmids were grown overnight in 5 ml LB + 20 mg l^{-1} Gentamycin, 50 mg l^{-1} kanamycin, 25 mg l^{-1} rifampicin and 2 mg l^{-1} tetracyclin. Cultures were spun down at 4,000 r.p.m. for 10 minutes and the bacterial pellet was resuspended in 1 ml MMAi (5 g l^{-1} Murashige and Skoog salts without vitamins, 2 g l^{-1} MES, 20 g l^{-1} sucrose, pH 5.6 and 0.2 mM Acetosyringone). The OD$_{600}$ was measured with a spectrophotometer. The infiltration samples were mixed 1/1 at a total OD$_{600}$ of 0.8. Samples were incubated at room temperature for 2 h and infiltrated into the underside of *Nicotiana benthamiana* leaves with a 1 ml syringe. After 2 days, leaf samples were cut out with a razor blade and imaged with a confocal microscope.

Protoplast transfection and FLIM measurements were performed on a Leica SP8 as described[41].

Structural homology modelling. SwissModel (https://swissmodel.expasy.org/) was used to model the structure of DIX-LIKE. To this end, the conserved N-terminal part of SOK1 was entered into the program and the software itself selected the best matching crystal structure, which was human Dvl2 (PBD: 4WIP).

Statistics and image editing. For all experiments involving transgenic lines, care was taken to analyse multiple independent transgenics, where lines were selected on the basis of whether they represented non-extreme characteristics. Only results representing most observations are shown. All sample and observation numbers are listed in Supplementary Table 3.

Raw microscopy images were collected, and brightness was uniformly modified across the entire image. When images were to be directly compared, brightness modifications were performed in an identical manner.

Reporting Summary. Further information on research design is available in the Nature Research Reporting Summary linked to this article.

Data availability

The data that support the findings of this study are available from the corresponding authors upon reasonable request.

References

1. Butler, M. T. & Wallingford, J. B. Planar cell polarity in development and disease. *Nat. Rev. Mol. Cell Biol.* **18**, 375–388 (2017).
2. Nakamura, M., Kiefer, C. S. & Grebe, M. Planar polarity, tissue polarity and planar morphogenesis in plants. *Curr. Opin. Plant. Biol.* **15**, 593–600 (2012).
3. St Johnston, D. & Ahringer, J. Cell polarity in eggs and epithelia: parallels and diversity. *Cell* **141**, 757–774 (2010).
4. Chiou, J.-G., Balasubramanian, M. K. & Lew, D. J. Cell polarity in yeast. *Annu. Rev. Cell. Dev. Biol.* **33**, 77–101 (2017).
5. St. Johnston, D. Establishing and transducing cell polarity: common themes and variations. *Curr. Opin. Cell Biol.* **51**, 33–41 (2018).
6. Yoshida, S. et al. Genetic control of plant development by overriding a geometric division rule. *Dev. Cell.* **29**, 75–87 (2014).
7. De Rybel, B. et al. A bHLH complex controls embryonic vascular tissue establishment and indeterminate growth in *Arabidopsis*. *Dev. Cell.* **24**, 426–437 (2013).
8. Gälweiler, L. et al. Regulation of polar auxin transport by AtPIN1 in *Arabidopsis* vascular tissue. *Science* **282**, 2226–2230 (1998).
9. Müller, A. et al. AtPIN2 defines a locus of *Arabidopsis* for root gravitropism control. *EMBO J.* **17**, 6903–6911 (1998).
10. Friml, J., Wiśniewska, J., Benková, E., Mendgen, K. & Palme, K. Lateral relocation of auxin efflux regulator PIN3 mediates tropism in *Arabidopsis*. *Nature* **415**, 806–809 (2002).
11. Friml, J. et al. Efflux-dependent auxin gradients establish the apical-basal axis of *Arabidopsis*. *Nature* **426**, 147–153 (2003).
12. Langowski, L. et al. Cellular mechanisms for cargo delivery and polarity maintenance at different polar domains in plant cells. *Cell Discov.* **2**, 16018 (2016).
13. Dong, J., MacAlister, C. A. & Bergmann, D. C. BASL controls asymmetric cell division in *Arabidopsis*. *Cell* **137**, 1320–1330 (2009).
14. Takano, J. et al. Polar localization and degradation of *Arabidopsis* boron transporters through distinct trafficking pathways. *Proc. Natl Acad. Sci.* **107**, 5220–5225 (2010).
15. Pillitteri, L. J., Peterson, K. M., Horst, R. J. & Torii, K. U. Molecular profiling of stomatal meristemoids reveals new component of asymmetric cell division and commonalities among stem cell populations in *Arabidopsis*. *Plant Cell* **23**, 3260–3275 (2011).
16. Kania, U., Fendrych, M. & Friml, J. Polar delivery in plants; commonalities and differences to animal epithelial cells. *Open Biol.* **4**, 140017 (2014).
17. Moller, B. & Weijers, D. Auxin control of embryo patterning. *Cold Spring Harb. Perspect. Biol.* **1**, a001545 (2009).
18. Hardtke, C. S. & Berleth, T. The *Arabidopsis* gene MONOPTEROS encodes a transcription factor mediating embryo axis formation and vascular development. *EMBO J.* **17**, 1405–1411 (1998).
19. Berleth, T. & Jürgens, G. The role of the monopteros gene in organising the basal body region of the *Arabidopsis* embryo. *Development* **118**, 575–587 (1993).
20. Möller, B. K. et al. Auxin response cell-autonomously controls ground tissue initiation in the early *Arabidopsis* embryo. *Proc. Natl Acad. Sci. USA* **114**, E2533–E2539 (2017).
21. Schlereth, A. et al. MONOPTEROS controls embryonic root initiation by regulating a mobile transcription factor. *Nature* **464**, 913–916 (2010).
22. Weijers, D. et al. An arabidopsis minute-like phenotype caused by a semi-dominant mutation in a RIBOSOMAL PROTEIN S5 gene. *Development* **128**, 4289–4299 (2001).
23. Scheres, B. et al. Mutations affecting the radial organisation of the *Arabidopsis* root display specific defects throughout the embryonic axis. *Development* **121**, 53–62 (1995).
24. Benfey, P. N. et al. Root development in *Arabidopsis*: four mutants with dramatically altered root morphogenesis. *Development* **119**, 57–70 (1993).
25. Radoeva, T., ten Hove, C. A., Saiga, S. & Weijers, D. Molecular characterization of *Arabidopsis* GAL4/UAS enhancer trap lines identifies novel cell type-specific promoters. *Plant Physiol.* **171**, 1169–1181 (2016).
26. Alassimone, J.., Naseer, S. & Geldner, N. . A developmental framework for endodermal differentiation and polarity. *Proc. Natl Acad. Sci. USA* **107**, 5214–5219 (2010).
27. Liao, C. Y. & Weijers, D. A toolkit for studying cellular reorganization during early embryogenesis in *Arabidopsis thaliana*. *Plant J.* **93**, 963–976 (2018).
28. Traverso, J. A. et al. Roles of N-terminal fatty acid acylations in membrane compartment partitioning: *Arabidopsis* h-type thioredoxins as a case study. *Plant Cell* **25**, 1056–1077 (2013).
29. Bienz, M. Signalosome assembly by domains undergoing dynamic head-to-tail polymerization. *Trends. Biochem. Sci.* **10**, 487–495 (2014).
30. Ehebauer, M. T. & Arias, A. M. The structural and functional determinants of the Axin and Dishevelled DIX domains. *BMC Struct. Biol.* **9**, 70 (2009).
31. Schwarz-Romond, T. et al. The DIX domain of Dishevelled confers Wnt signaling by dynamic polymerization. *Nat. Struct. Mol. Biol.* **14**, 484–492 (2007).
32. Mansfield, C. et al. Ectopic BASL reveals tissue cell polarity throughout leaf development in *Arabidopsis thaliana*. *Curr. Biol.* **28**, 2638–2646 (2018).
33. Fukaki, H. et al. Genetic evidence that the endodermis is essential for shoot gravitropism in *Arabidopsis thaliana*. *Plant J.* **14**, 425–430 (1998).
34. Helariutta, Y. et al. The SHORT-ROOT gene controls radial patterning of the *Arabidopsis* root through radial signaling. *Cell* **101**, 555–567 (2000).
35. De Rybel, B. et al. A versatile set of ligation-independent cloning vectors for functional studies in plants. *Plant Physiol.* **156**, 1292–1299 (2011).
36. Weijers, D., Van Hamburg, J. P, Van Rijn, E., Hooykaas, P. J. & Offringa, R. Diphtheria toxin-mediated cell ablation reveals interregional communication during *Arabidopsis* seed development. *Plant Physiol.* **133**, 1882–1892 (2003).
37. Llavata-Peris, C., Lokerse, A., Moller, B., De Rybel, B. & Weijers, D. Imaging of phenotypes, gene expression, and protein localization during embryonic root formation in *Arabidopsis*. *Methods Mol. Biol.* **959**, 137–148 (2013).
38. Marhavý, P. et al. Targeted cell elimination reveals an auxin-guided biphasic mode of lateral root initiation. *Genes Dev.* **30**, 471–483 (2016).
39. von Wangenheim, D. et al. Live tracking of moving samples in confocal microscopy for vertically grown roots. *eLife* **6**, e26792 (2017).
40. de Reuille, P. B. et al. MorphoGraphX: A platform for quantifying morphogenesis in 4D. *eLife* **4**, 05864 (2015).
41. Rios, A. F., Radoeva, T., De Rybel, B., Weijers, D. & Borst, J. W. FRET-FLIM for visualizing and quantifying protein interactions in live plant cells. *Methods Mol. Biol.* **1497**, 135–146 (2017).

Author contributions

D.W. conceived the study. S.Y. performed most of the experiments under the supervision of D.W. and with help from A.v.d.S., L.v.G. and S.S. M.v.D. carried out the BiFC and FRET-FLIM experiments, SOK1 localization in ground tissue and in *shr* and *scr* mutants (together with C.A.t.H.) and SOK1/SOK5 swaps. B.M. initiated the project and identified the *SOK1* gene. M.A. and R.S. performed 3D SOK1 localization analysis. P.M. helped to perform live imaging under J.F.'s supervision. S.Y. and D.W. wrote the manuscript with input from all authors.

Competing interests

The authors declare no competing interests.

Additional information

Supplementary information is available for this paper at https://doi.org/10.1038/s41477-019-0363-6.

Reprints and permissions information is available at www.nature.com/reprints.

Correspondence and requests for materials should be addressed to S.Y. or D.W.

Journal peer review Information Nature Plants thanks Marie Barberon, Dominique Bergmann, Juan Dong and Markus Grebe for their contribution to the peer review of this work

Publisher's note: Springer Nature remains neutral with regard to jurisdictional claims in published maps and institutional affiliations.

Corresponding author(s):   Saiko Yoshida, Dolf Weijers

Reporting Summary

Nature Research wishes to improve the reproducibility of the work that we publish. This form provides structure for consistency and transparency in reporting. For further information on Nature Research policies, see Authors & Referees and the Editorial Policy Checklist.

Statistical parameters

When statistical analyses are reported, confirm that the following items are present in the relevant location (e.g. figure legend, table legend, main text, or Methods section).

n/a	Confirmed	
☐	☒	The exact sample size (n) for each experimental group/condition, given as a discrete number and unit of measurement
☐	☒	An indication of whether measurements were taken from distinct samples or whether the same sample was measured repeatedly
☒	☐	The statistical test(s) used AND whether they are one- or two-sided *Only common tests should be described solely by name; describe more complex techniques in the Methods section.*
☒	☐	A description of all covariates tested
☒	☐	A description of any assumptions or corrections, such as tests of normality and adjustment for multiple comparisons
☒	☐	A full description of the statistics including central tendency (e.g. means) or other basic estimates (e.g. regression coefficient) AND variation (e.g. standard deviation) or associated estimates of uncertainty (e.g. confidence intervals)
☒	☐	For null hypothesis testing, the test statistic (e.g. F, t, r) with confidence intervals, effect sizes, degrees of freedom and P value noted *Give P values as exact values whenever suitable.*
☒	☐	For Bayesian analysis, information on the choice of priors and Markov chain Monte Carlo settings
☒	☐	For hierarchical and complex designs, identification of the appropriate level for tests and full reporting of outcomes
☒	☐	Estimates of effect sizes (e.g. Cohen's d, Pearson's r), indicating how they were calculated
☒	☐	Clearly defined error bars *State explicitly what error bars represent (e.g. SD, SE, CI)*

Our web collection on statistics for biologists may be useful.

Software and code

Policy information about availability of computer code

Data collection	No specialized software was used for data collection
Data analysis	No specialized software was used for data analysis

For manuscripts utilizing custom algorithms or software that are central to the research but not yet described in published literature, software must be made available to editors/reviewers upon request. We strongly encourage code deposition in a community repository (e.g. GitHub). See the Nature Research guidelines for submitting code & software for further information.

Data

Policy information about availability of data

All manuscripts must include a data availability statement. This statement should provide the following information, where applicable:

- Accession codes, unique identifiers, or web links for publicly available datasets
- A list of figures that have associated raw data
- A description of any restrictions on data availability

The data that support the findings of this study are available from the corresponding author upon reasonable request.

Field-specific reporting

Please select the best fit for your research. If you are not sure, read the appropriate sections before making your selection.

☒ Life sciences   ☐ Behavioural & social sciences   ☐ Ecological, evolutionary & environmental sciences

For a reference copy of the document with all sections, see nature.com/authors/policies/ReportingSummary-flat.pdf

Life sciences study design

All studies must disclose on these points even when the disclosure is negative.

Sample size	A full list of sample sizes is included as Extended Table 3. These sample numbers were chosen according to common standards in the field
Data exclusions	No data points were excluded
Replication	Each experiment was repeated at least twice, and only results representing the consistent outcome are reported.
Randomization	All independent transgenic lines were randomly picked, and all individuals for analysis were likewise randomly picked.
Blinding	Given that comparisons are generally qualitative in nature, blinding was not relevant.

Reporting for specific materials, systems and methods

Materials & experimental systems

n/a	Involved in the study
☐	☒ Unique biological materials
☒	☐ Antibodies
☒	☐ Eukaryotic cell lines
☒	☐ Palaeontology
☒	☐ Animals and other organisms
☒	☐ Human research participants

Methods

n/a	Involved in the study
☒	☐ ChIP-seq
☒	☐ Flow cytometry
☒	☐ MRI-based neuroimaging

Unique biological materials

Policy information about availability of materials

Obtaining unique materials	All unique biological materials (plasmids and transgenic Arabidopsis lines) are available without restrictions from the corresponding authors.